

FAST EYE DETECTOR USING METRIC LEARNING FOR IRIS ON THE MOVE

Yuka Ogino, Takahiro Toizumi and Masato Tsukada

NEC Corporation

ABSTRACT

This paper proposes a fast eye detection method based on fully-convolutional Siamese networks for iris recognition. The iris on the move system requires to capture high resolution iris images from a moving subject for iris recognition. Therefore, capturing images contains both eyes at high-frame-rate increases the chance of iris imaging. In order to output the authentication result in real time, the system requires a fast eye detector extracting the left and right eye regions from the image. Our method extracts features of a partial face image and a reference eye image using Siamese network frameworks. Similarity heat maps of both eyes are created by calculating the spatial cosine similarity between extracted features. Besides, we use CosFace as a loss function for training to discriminate the left and right eyes with high accuracy even with a shallow network. Experimental results show that our method trained by CosFace is fast and accurate compared with conventional generic object detection methods.

Index Terms— Iris recognition, image acquisition, image processing

1. INTRODUCTION

Iris recognition is known as one of the most accurate biometric authentication methods. In general, iris recognition [1] involves an iris localization process and feature extraction process. The iris localization process cuts out the annular structure of the iris region with inner and outer circles. The feature extraction process extracts features from the iris region for matching. Iris recognition requires a very high resolution iris image with 10–15.7 pixels per millimeter [2, 3]. To expand the application of iris recognition, advanced iris imaging methods are required. Iris imaging methods to capture not only one eye but also both eyes in a partial face region have been proposed [4].

Partial face capturing can shorten the imaging time without precise control to adjust to one eye of a subject. In addition, capturing the region of interest (ROI) a whole face reduces the load on communication and processing speeds, and can improve the frame rate while keeping the resolution high. In systems that capture the iris of a moving person, such as iris at a distance (IAAD) and iris on the move (IOTM) [4, 5, 6],

capturing partial face images at a high frame rate increases the chance of iris imaging with a moving subject.

The IOTM system requires iris recognition from partial face images acquired at high frame rates. Iris localization is not suitable for partial face images because it is designed for images of one eye. The system requires fast extraction of the left and right eyes from a partial face images in real time.

To develop an eye detector for IOTM systems, we defined three requirements. First, the detector must process images in real time. Second, the detector must be able to accurately distinguish between the left and right eyes. Finally, the detector must be accurate enough to crop the iris within an image area. For example, an iris with a diameter of 160 pixels should almost fit within the VGA size. We assume that an input image always contains the left and right eyes and that the resolution is fixed to 10–15.7 pixels per millimeter.

In this paper, we propose an eye detector for fast and accurate extraction of the left and right eyes from a partial face image captured by the IOTM system. We focus on metric learning methods. The proposed method is based on fully-convolutional Siamese networks (SiamFC) [7], and it extracts features from a single eye image as a reference, and the partial face image as a search target. Our detector generates heat maps by calculating the spatial cosine similarity between the features. During training, we apply CosFace [8] to the loss function. It is possible to distinguish the right eye from the left eye with high accuracy even with a shallow network. We evaluate proposed method using public datasets. The experimental results show that our method is faster and more accurate than other well-known object detection methods.

2. RELATED WORK

The ideal for eye detection is to develop an algorithm that achieves the three goals of high accuracy, high robustness and high speed. Conventional eye detection methods are classified into three categories: hand crafted feature-based methods, template-based methods and CNN-based methods.

The hand-crafted feature-based detectors [9, 10, 11, 12] have used local image features and classifiers such as SVM. Gabor filters or HOG features have been used as local image features. The template-based methods have generated eye templates by using trained filters such as correlation filters [13, 14, 15]. These methods are fast with a few tens of

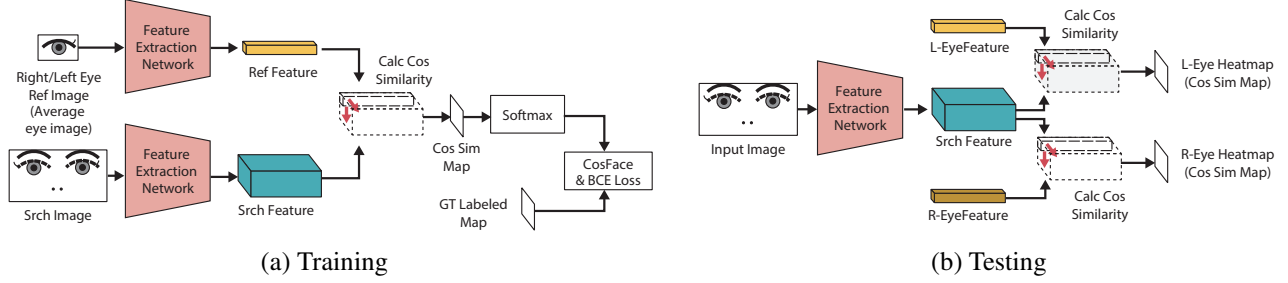


Fig. 1. Training and test frameworks of proposed method. (a) Training framework. Reference and search images are fed into same feature extractor. Heat map is generated by calculating spatial cosine similarity between extracted features. Networks are optimized by the binary cross entropy (BCE) loss with CosFace as shown in Eq. 2. (b) Testing framework. Detector computes spatial cosine similarity between pre-featured reference features and extracted search feature.

milliseconds processing time. However, they are sensitive to environmental changes in images.

Recently, CNN techniques have emerged as powerful methods for object detection [16, 17]. These methods, called generic object detection methods [18], detect and recognize objects of different scales and classes. Faster R-CNN [16] is one of the methods for generic object detection. This method generates a feature map from an input image by using convolutional layers and estimates ROIs with high objectness using a region proposal network. Then, a fully connected layer outputs the object class and bounding box of the ROIs. Nasaif et al. [19] proposed FRCNN-GNB for eye detection. They use Faster R-CNN [16] to detect initial eye regions and then apply Gabor filters and a naïve Bayes model for the final eye detection. CNN-based methods are robust to the image environment, but they lack real-time performance due to the processing time. To speed up the processing time of a CNN model, Li et al. [20] detect eye candidates from a local image gradient and classify the candidate regions into left, right and eye conditions using shallow CNN models.

As an end-to-end fast eye detection method for CNN models, we focus on fully-convolutional Siamese networks (SiamFC) [7]. The SiamFC is an object tracker that has achieved high performance and speed in the Visual Object Tracking (VOT) challenge. It extracts features from input reference and search images by using common networks. Then, a similarity score map is generated using the the correlation of the extracted reference and search features. SiamFC detects the position of a reference object in a search image by thresholding the similarity score map.

3. PROPOSED METHOD

3.1. Framework

We consider SiamFC [7] to be a two-class classifier that determines whether a subregion of a search feature is a tracking target or not. To use SiamFC as an eye detector, we design a new loss function to generate discriminative features between

right and left eyes. We apply a margin on hot labels using CosFace [8] to separate the target classes from others.

We define the reference image as I_{ref} and the search image as I_{srch} . The same CNN feature extractors ϕ calculate features from these two images. The features of I_{ref} and I_{srch} are defined as $f_{ref} := \phi(I_{ref}) \in \mathbb{R}^{m \times n \times c}$ and $F_{srch} := \phi(I_{srch}) \in \mathbb{R}^{M \times N \times c}$, respectively. The numbers of channels c in F_{srch} and f_{ref} are equal, but each has a different spatial size. Let $F_{srch}[u] \in \mathbb{R}^{m \times n \times c}$ denote the partial region of size $m \times n \times c$ at spatial position $u \in U$ of feature F_{srch} .

Figure 1 shows the frameworks of the proposed method. In training, I_{ref} is fixed to a single average image of one eye, and the same image is flipped between the left and right eyes. We assume that I_{srch} always includes both eyes, and learn detection tasks for the left and right eyes, respectively. In testing, the same I_{ref} as in training is used to obtain both features f_{refR} and f_{refL} in advance. The peak position of the output heat map is scaled and output as detection results.

3.2. Similarity Map

The proposed method calculates the kernel-wise cosine similarity between $F_{srch}[u]$ and f_{ref} , and obtains similarity heat map Q . The edge of F_{srch} is replicated before calculating the cosine similarity so that Q has the same spatial size (M, N) as F_{srch} . The cosine similarity at spatial position u on heat map Q can be calculated as

$$Q[u] = \cos \theta_u = \frac{f_{ref} \cdot F_{srch}[u]}{\|f_{ref}\|_2 \|F_{srch}[u]\|_2}. \quad (1)$$

3.3. Loss Function

We design a loss function based on binary cross entropy (BCE) with CosFace [8] to accurately classify one side of the eye (2 classes) from others. CosFace has a margin parameter m applied only to the positive label locations and the scale parameter s . These parameters encourages cosine decision margin between classes. In the case of a right eye class,

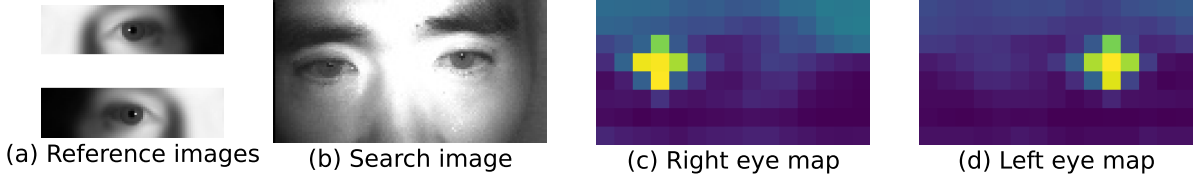


Fig. 2. Examples of input images and output heat maps. (a) Reference images (average images of both eye regions). (b) Search image (partial face image) sampled from Casia-Iris-M1-S2 dataset. (c)(d) Inferred heat maps of left and right eyes.

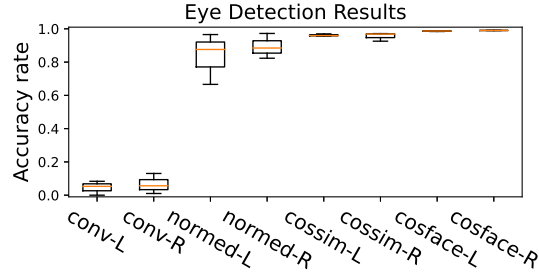


Fig. 3. Accuracy distribution of ablation study. We trained our model three times for each condition. Conditions include only convolution (conv), with normalization (normed), with cosine similarity (cossim) and with CosFace (cosface). L and R are the results for left and eyes.

CosFace is expected to separate the feature distribution of the right eye class from that of the left eye class. The total loss function L based on the BCE is given by

$$L = -\frac{1}{|U|} \sum_{u \in U} \{ y_u \log \frac{e^{s(Q_u - m)}}{e^{s(Q_u - m)} + \sum_{t \neq u} e^{sQ_t}} + (1 - y_u) \log \frac{e^{sQ_u}}{e^{s(Q_u - m)} + \sum_{t \neq u} e^{sQ_t}} \}. \quad (2)$$

4. EXPERIMENTAL RESULTS

In this section, we show two experiments done to evaluate the performance of the proposed method. The first was an ablation study to confirm the contributions of the proposed conditions (cosine similarity and CosFace). The second was a comparison between the proposed method and generic object detection methods.

We used a single network architecture for both experiments. The base network for SiamFC was modified from ResNet [21] as shown in Table 1. The differences from the original ResNet are single channel input and the number of layers. Each layer contained convolution, batch normalization and ReLU activation. For training the model, we used stochastic gradient descent (SGD) as the optimizer. The learning rate was 0.1 on the first epoch and switches to 0.01

from the second epoch. The weight decay was 0.0001. The batch size was 128 for each iteration, and the total number of iteration is 11k and 1k iterations (50 and 70 epochs) for the ablation study and the comparison. The CosFace parameters (m, s) were (0.3, 30).

The input image is scaled down from the original size, with the resolution of the iris diameter at about 10 pixels. The parameter α is the scale ratio between the original image and the similarity heat map. The value of α depends on the dataset. In the case of Casia-Iris-M1-S1 [22], we used $\alpha = 80$ to scale down the input image. Reference images and a sample of a partial face image are shown in Figs. 2 (a) and (b). Inferred heat maps are shown in Figs. 2 (c) and (d). The ground truth heat map is a binary map labelled on the eye center pixel and its four neighbour pixels.

4.1. Ablation Study

We evaluated the proposed method under four conditions to check the contributions of each component: (1) direct convolution of F_{srch} with f_{ref} (conv) which is equivalent to SiamFC [7], (2) convolution of pixel-wise normalized F_{srch} and f_{ref} (normed), (3) convolution of kernel-wise normalized cosine similarity between $F_{srch}[u]$ and f_{ref} (cossim), and (4) convolution of kernel-wise normalized cosine similarity with CosFace (cosface).

For the ablation study, we prepared training and test datasets using approximately 60,000 partial face images. The datasets included Casia-Iris-M1-S1 [22], Casia-Iris-Distance [23] and our own dataset. We manually annotated the ground truth for each dataset. The annotated dataset were split into 50% for training and the remaining 50% for testing. We trained the model on each condition three times with the same parameters.

We evaluated the detected coordinates with or without half of the VGA size from the ground truth positions. (i.e., whether or not the detected coordinates were within the margin of the iris diameter from the center of the ground-truth VGA image). In the evaluation, we calculated criteria $T(\mathbf{x}, \alpha\hat{\mathbf{x}})$ per image given by

$$T(\mathbf{x}, \hat{\mathbf{x}}) = \begin{cases} 1, & \text{if } ((W - r) < |x - \alpha\hat{x}|) \\ & \& ((H - r) < |y - \alpha\hat{y}|), \\ 0, & \text{otherwise} \end{cases} \quad (3)$$

Table 1. Network architecture

	input	layer1	layer2	layer3	layer4	layer5
convlayer	$[7 \times 7, 32]$ stride 2	$[3 \times 3, 32] \times 2$ $[3 \times 3, 32]$ stride 1	$[3 \times 3, 32] \times 2$ $[3 \times 3, 32]$ stride 1	$[3 \times 3, 32] \times 2$ $[3 \times 3, 32]$ stride 1	$[3 \times 3, 32] \times 2$ $[3 \times 3, 32]$ stride 1	$[3 \times 3, 128] \times 2$ $[3 \times 3, 128]$ stride 1
pooling		maxpool 2×2 , stride 2		maxpool 2×2 , stride 2		

where $\hat{\mathbf{x}} = (\alpha\hat{x}, \alpha\hat{y})$ are the detected coordinates enlarged to the original scale and $\mathbf{x} = (x, y)$ is the ground truth. The margin parameter is $r = 75$ and the (H, W) are half the size of the VGA (320, 240). We used the average ratio of $T(\mathbf{x}, \alpha\hat{\mathbf{x}})$ in the test dataset as an evaluation metric.

Figure 3 shows the resulting distributions of the detection accuracy for each condition. The result for “conv” showed almost no progress in training, and the accuracy rate was under 10%. “Normed” improved the accuracy dramatically over “conv” and achieved an accuracy over 70%. This is because “normed” makes the search feature closer to the reference feature. However, there are variations between the left and right results. The accuracy was further improved by applying “cos-sim” and “cosface”. These accuracies were stable and exceeded 90%. “Cosface” achieved the highest accuracy with the least variation in all conditions. These results confirm that kernel-wise normalization and CosFace play an important role in the proposed method.

4.2. Comparison with Generic Object Detection Methods

We compared the proposed method with generic object detection methods: FRCNN [16] and YOLOv5 (a PyTorch implementation of [24]). We re-trained YOLO and FRCNN models to detect both eyes from partial face images. The proposed method and YOLO were trained in 70 epochs, while FRCNN was trained in 5 epochs because the training time of FRCNN is much longer than the other methods.

For comparison, we classified the manually annotated datasets into training and untraining domains to evaluate the domain robustness of the proposed method. The training domain datasets included Casia-Iris-Distance [23] and Casia-Iris-M1-S1 [22]. We trained 50% of the images from the training domain datasets. The other 50% of the training domain datasets was utilized in the evaluation (trained domain). The untraining domain datasets included Casia-Iris-M1-S2 [22] and Casia-Iris-M1-S3 [22]. All of the untraining domain datasets (untrained domain) were used for evaluation.

We compared the three methods using the F1 score. Since the proposed method assumes that both eyes are always included in an input image, a false positive (FP) is always equal to a false negative (FN). This assumption makes the precision equal to the recall for the proposed method. In generic object detection, the number of detection targets is unlimited, so YOLO and FRCNN may detect more targets than expected

Table 2. Comparison between proposed method and generic object detection methods. “Trained domain” is result for dataset with same domain as training dataset. “Untrained domain” is result for datasets with different domain from training. “Time” is average time taken to process input image of 96 \times 123 pixels 10 times in CPU environment.

		Proposed	YOLOv5	FRCNN
Trained	Right	0.998	0.983	0.999
domain	Left	0.981	0.984	0.998
Untrained	Right	0.993	0.660	0.980
domain	Left	0.956	0.608	0.982
Time[ms]		21	87	1970

(the FN may differ from the FP). Thus, we needed to evaluate them on the basis of the F1 score instead of accuracy.

Table 2 shows the result of the comparison. The results obtained for the trained domain datasets show that FRCNN had the highest accuracy, but the accuracy of the proposed method was almost the same as FRCNN. The results obtained using the untrained domain datasets (Table 2, Untrained) show that the proposed method and the FRCNN maintained high accuracy for both eyes. This confirms that the proposed method and FRCNN have robustness to the domain difference between training and test datasets. In terms of execution time in the CPU environment (Intel Core i9-9900 @ 3.60 GHz), the proposed method was the fastest among the three methods with a 21-ms processing time for an the average of 10 times of processing for a partial face image of 96 \times 123 pixels. These results confirm that our proposed method achieved higher accuracy with a higher calculation speed than the other generic object detection methods.

5. CONCLUSION

This paper proposed a fast eye detection method based on fully-convolutional Siamese networks for partial face images. By applying a loss function with CosFace during training, a shallow network was able to discriminate between the left and right eyes with high accuracy. Experimental results showed that CosFace is effective in achieving high speed and high accuracy, and our method is faster and more accurate in a CPU environment compared with conventional generic object detection methods.

6. REFERENCES

- [1] J.Daugman et al., “Probing the uniqueness and randomness of iriscodes: Results from 200 billion iris pair comparisons,” *Proceedings of the IEEE*, vol. 94, no. 11, pp. 1927–1935, 2006.
- [2] “Information technology — extensible biometric data interchange formats — part 6: Iris image data,” 2021.
- [3] “Information technology — biometric sample quality — part 6: Iris image data,” *ISO/IEC 29794-6:2015*, 2015.
- [4] K. Nguyen et al., “Long range iris recognition: A survey,” *Pattern Recognition*, vol. 72, pp. 123–143, 2017.
- [5] J.Matey et al., “Iris on the move: Acquisition of images for iris recognition in less constrained environments,” *Proc. of the IEEE*, vol. 94, no. 11, pp. 1936–1947, 2006.
- [6] K.Zhang et al., “All-in-focus iris camera with a great capture volume,” in *2020 IEEE International Joint Conference on Biometrics (IJCB)*. IEEE, 2020, pp. 1–9.
- [7] L. Bertinetto et al., “Fully-convolutional siamese networks for object tracking,” in *European conference on computer vision*. Springer, 2016, pp. 850–865.
- [8] H. Wang et al., “Cosface: Large margin cosine loss for deep face recognition,” in *Proc. of the IEEE Conf. on CVPR*, 2018, pp. 5265–5274.
- [9] S. Chen et al., “Eye detection using discriminatory haar features and a new efficient svm,” *Image and Vision Computing*, vol. 33, pp. 68–77, 2015.
- [10] R. Sharma et al., “Lean histogram of oriented gradients features for effective eye detection,” *Journal of Electronic Imaging*, vol. 24, no. 6, pp. 063007, 2015.
- [11] V. Laxmi et al., “Eye detection using gabor filter and svm,” in *Proc. of Int'l Conf. on ISDA*. IEEE, 2012, pp. 880–883.
- [12] S. Kawato et al., “Real-time detection of between-the-eyes with a circle frequency filter,” in *Proc. of IEEE Conf. on ACCV*. Citeseer, 2002, vol. 2, pp. 442–447.
- [13] David S Bolme, Bruce A Draper, and J Ross Beveridge, “Average of synthetic exact filters,” in *IEEE Conference on Computer Vision and Pattern Recognition (CVPR)*. IEEE, 2009, pp. 2105–2112.
- [14] G. M.Araujo et al., “Fast eye localization without a face model using inner product detectors,” in *IEEE International Conference on Image Processing (ICIP)*. IEEE, 2014, pp. 1366–1370.
- [15] M. Leo et al., “Unsupervised approach for the accurate localization of the pupils in near-frontal facial images,” *Journal of Electronic Imaging*, vol. 22, no. 3, pp. 033033, 2013.
- [16] S. Ren et al., “Faster r-cnn: Towards real-time object detection with region proposal networks,” *Advances in neural information processing systems*, vol. 28, pp. 91–99, 2015.
- [17] J. Redmon et al., “Yolov3: An incremental improvement,” *arXiv preprint arXiv:1804.02767*, 2018.
- [18] L. Liu et al., “Deep learning for generic object detection: A survey,” *International journal of computer vision*, vol. 128, no. 2, pp. 261–318, 2020.
- [19] A. K. Nsaif et al., “Frcnn-gnb: Cascade faster r-cnn with gabor filters and naïve bayes for enhanced eye detection,” *IEEE Access*, vol. 9, pp. 15708–15719, 2021.
- [20] B. Li et al., “Real time eye detector with cascaded convolutional neural networks,” *Applied Computational Intelligence and Soft Computing*, vol. 2018, 2018.
- [21] K. He et al., “Deep residual learning for image recognition,” in *Proc. of the IEEE Conf on CVPR*, 2016, pp. 770–778.
- [22] T. Tan et al., “Casia-iris-m1,” 2012, <http://biometrics.idealtest.org/dbDetailForUse>
- [23] T. Tan et al., “Casia-iris-distance,” 2012, <http://biometrics.idealtest.org/dbDetailForUse>
- [24] A. Bochkovskiy et al., “Yolov4: Optimal speed and accuracy of object detection,” *arXiv preprint arXiv:2004.10934*, 2020.